Proceedings of the 21st ICSMGE, Vienna, Austria, 14 – 19 June 2026. Pistrol, Adam & Schweiger (eds.)
Published by: ÖGG, Austrian Society for Geomechanics, Salzburg, Austria, ISBN 978-3-9503898-4-5
https://doi.org/10.53243/ICSMGE2026-1217

Impact of Loose Sand Layers on the Lateral Capacity of Offshore Wind Turbine Monopiles on Inclined Seabed

Hadi Valizadeh, S. Feyza Çinicioğlu
Özyeğin University, Istanbul, Turkey, hadi.valizadeh@ozyegin.edu.tr

Özer Çinicioğlu
Bogazici University, Istanbul, Turkey

ABSTRACT: Monopiles are widely used in offshore engineering for structures such as offshore wind turbines and nearshore wharves. However, the complexity of the seabed and the effects of scouring can lead to sloping ground conditions, which reduce the lateral bearing capacity of the monopile by diminishing the subgrade reaction modulus. Geotechnical and geophysical surveys of operational offshore wind farms reveal that the seabed often consists of layered sand profiles or interbedded sand and clay layers. Despite this prevalence, the lateral behavior of monopiles in layered soils remains insufficiently understood, as most previous studies have focused on homogeneous sand or clay conditions. This study explores the effect of loose sand interlayers on the lateral capacity of large-diameter monopiles embedded in an inclined seabed. Forty finite element analyses were performed using the Hardening Soil Small Strain model, calibrated and validated through element-scale, field, and centrifuge tests. The simulations captured stress-dependent stiffness degradation and small-strain behavior. Ten configurations of loose sand (Dr = 30%) within dense sand (Dr = 70%) were analyzed, varying in depth and thickness. Additionally, four seabed slopes were considered to assess their influence on monopile performance under monotonic loading. Results reveal that seabed slope and loose sand layer configuration significantly influence monopile lateral performance. The initial stiffness, ultimate lateral capacity, and the depth of the pivot point of the monopile change depending on the position and thickness of the sand layers. While monopiles in flat, homogeneous seabeds exhibit the best performance, weakening of the top sand layer causes the greatest reduction in stiffness and ultimate capacity. In contrast, mid- and bottom-layer weakening preserves more stiffness, yet still decreases overall capacity. Moreover, steeper seabed slopes deepen the pivot point and amplify instability, highlighting the importance of accounting for soil stratification and seabed geometry in design.

KEYWORDS: Offshore wind turbines, Monopiles, Lateral capacity, Stiffness degradation, Sandy soils, Inclined seabed.

1 INTRODUCTION

Sloping seabed are common in offshore environments due to natural seabed irregularities and hydrodynamic actions such as erosion, which can occur even after the installation of offshore structures. These conditions may significantly influence soil–structure interaction (SSI), making it essential to assess the stability and performance of foundations under sloping seabed scenarios compared to flat seabed conditions. Monopile foundations, widely used in offshore wind farms, are particularly relevant in this context. These foundations consist of large-diameter steel piles, typically ranging from 5–6 m for regular monopiles to 6–8 m for XL and up to 13 m or more for XXL monopiles, making their interaction with sloping seabeds a critical design consideration.

The influence of sloping ground on laterally loaded piles has been widely studied through analytical, experimental, and numerical approaches. Early work by Gabr and Borden (1990) provided theoretical solutions, while centrifuge and model tests (Mezazign & Levacher, 1998; Muthukkumaran, 2008, 2014; Sivapriya & Gandhi, 2011) demonstrated that slope angle, crest distance, and soil properties significantly affect p–y behavior and lateral capacity. Full-scale tests (Mirzoyan, 2007) and 3D finite element (FE) analyses (Chae et al., 2004; Georgiadis & Georgiadis, 2010, 2012) confirmed that slopes reduce lateral resistance and increase bending moments, leading to modified p–y curves and analytical formulations. Recent research has advanced understanding through large-scale tests and refined models. Nimityongskul et al. (2017) examined pile response at varying distances from slope crests, while Chandaluri & Sawant (2018) used PLAXIS 3D to assess the effects of pile diameter, slope angle, and soil mechanical properties. Peng et al. (2019) introduced a modified strain wedge model validated by in-situ tests. Lin et al. (2022) proposed an equivalent wedge-based method for piles near sand slopes, showing that ultimate soil resistance decreases with slope height. Yue et al. (2024) investigated cyclic lateral loading on sloping ground, revealing that downslope loading amplifies displacement and bending moments, with responses strongly influenced by cyclic loading ratio (CLR) rather than static load ratio.

Geotechnical surveys from offshore wind farms located in North Sea consistently show that the seabed is composed of layered sands and alternating sand-clay formations. According to Sánchez et al. (2019), 21.7% of monopile foundations across 69 wind farms were placed in these layered soil conditions, yet the lateral performance of monopiles in such stratified soils remains poorly understood due to the predominance of research focused on uniform sand or clay substrates. Hu et al. (2022) used 3D FE modeling to examine lateral resistance in two-layer sand profiles. Their results demonstrated that variations in top-layer thickness and the presence of a thin loose-sand layer within a dense-sand profile significantly influence monopile lateral capacity. Haiderali and Madabhushi (2024) demonstrated through 3D FE analyses that loose sand layers within dense sand significantly reduce the lateral capacity of XXL monopiles, with an effect strongly dependent on the layer's thickness and depth. These findings underscore the complexity of pile behavior on sloping ground and the need for further research on offshore monopiles under combined sloping seabed and layered soil conditions.

This study investigates the combined effect of loose sand layers and seabed inclination on the lateral response of extra-large monopiles using 3D FE modeling in PLAXIS. Building on previous work focused solely on soil layering, this research introduces sloping seabed conditions to evaluate their interaction with layered profiles. Forty simulations reveal a consistent relationship between slope, loose layer configuration, and lateral performance, highlighting variations in initial stiffness, ultimate capacity, and pivot depth. The findings strengthen design insights by showing how slope-induced instability and soil stratification critically influence load transfer and rotational behavior in offshore monopile systems.

2 NUMERICAL SIMULATION

PLAXIS 3D (Plaxis, 2024) was employed for its advanced capability to model complex SSI, including nonlinear soil behavior, layered profiles, and detailed soil–foundation interfaces. The Hardening Soil model with small-strain stiffness (HSS) (Benz 2007) was adopted to capture realistic soil response, as it accounts for stiffness degradation and stress dependency, overcoming the limitations of elastic-perfectly plastic models such as Mohr–Coulomb. The HSS model incorporates the Matsuoka–Nakai failure criterion and a Drucker–Prager plastic potential, with a hyperbolic stress–strain relationship.

2.1 *Validation Analysis*

Model validation was performed using a multi-scale approach, including element-level triaxial tests, centrifuge modeling, and large-scale field data to ensure the reliability of the numerical simulations. The HSS model in PLAXIS 3D accurately reproduced stress–strain and volumetric responses of Fontainebleau sand (Latini & Zania 2017) at different densities, confirming its capability to capture stiffness variation, peak strength, and contractive-to-dilative behavior (Figure 1). The 3D numerical simulation was validated against two benchmark studies: a full-scale field test by Reese et al., (1974) and a centrifuge test by Georgiadis et al., (1992), covering different soil and groundwater conditions. The simulation results closely matched the experimental lateral load responses (H–y/D curves), as shown in Figure 2, confirming the reliability of the HSS model.

3 PARAMETRIC NUMERICAL ANALYSIS

A symmetry plane was applied in PLAXIS 3D to model half of the domain, reducing computational effort (Figure 3). The mesh combined hexahedral and tetrahedral elements, with size varying by model.

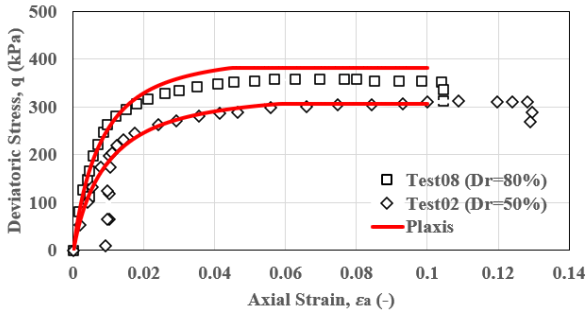

(a)

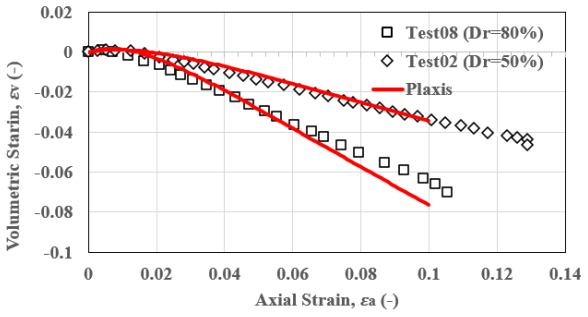

(b)

Figure 1. Single element simulations of drained triaxial compression tests by Latini & Zania (2017), a) q-ε_a curve, b) $\varepsilon_v - \varepsilon_a$ curve.

Boundary conditions followed PLAXIS recommendations: the bottom fixed at 2L depth, and lateral boundaries placed at 12D longitudinally and 4D transversely (L is defined as the pile embedment length, and D as the pile diameter). Convergence and sensitivity analyses confirmed adequacy. The pile was modeled as linear-elastic steel (E = 210 GPa, ν = 0.3) using six-noded plate elements, while 12-noded interface elements simulated pile–soil interaction with slip and separation governed by the HSS model.

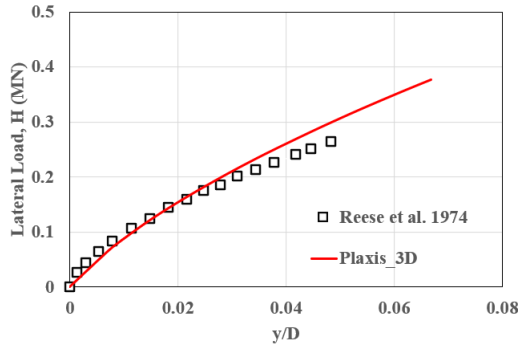

(a)

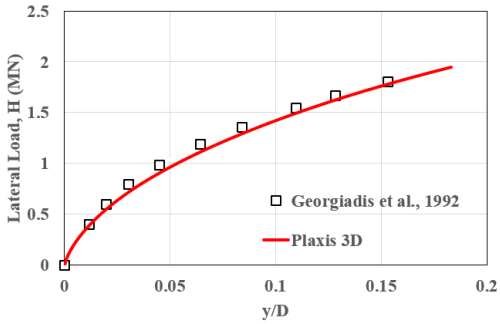

(b)

Figure 2. H-y/D results from the 3D FE analyses compared with the messured results, a) Reese et al. (1974), b) Georgiadis et al. (1992).

Bottom boundaries were fixed in all directions, and side boundaries allowed vertical movement (Figure 3a).

A pile diameter of 10 m was selected, representing XXL monopiles, with thickness calculated using the American Petroleum Institute (API) (API 2014) formula t=0.006+D/100 (m). The embedded length was set at 30 m, yielding an L/D ratio of 3. Relative density values of 30% and 70% were used to represent loose (LS) and dense (DS) sand, respectively, with corresponding friction angles of 30° and 39°, derived from Meyerhof's (1959) correlation φ=28+0.15Dr. These parameters reflect realistic marine sand conditions, ensuring the reliability of the lateral capacity assessment. Sand properties are summarized in Table 1. To assess seabed slope effects, inclinations of 5%, 10%, and 15% were modeled and compared with a flat seabed condition. Additionally, the influence of loose sand layers was examined by positioning them at the top, middle, and bottom thirds of the embedded pile length, with thicknesses of L/15, L/6, and L/3 (Figure 4). To simulate realistic offshore loading conditions, a normalized load eccentricity of h/D=10 was adopted, representing a balance between wind- and wave-dominated scenarios (Byrne et al., 2020). Figure 4d presents the titles and corresponding descriptions of the selected models.

The soil–pile relative stiffness factor (S) was determined using the formulation proposed by Poulos and Hull (1989). According to this formula, the stiffness factor is calculated as $S = (E_P I_P / E_S L^4)$, where Es is the average Young's modulus

of soil between the ground surface and the embedded depth. This factor characterizes pile rigidity: values below 0.0025 indicate flexible behavior, values above 0.208 represent rigid behavior, and intermediate values correspond to semi-rigid piles. All samples were classified as rigid or semi-rigid monopiles based on their relative stiffness characteristics.

4 DISSCUSSION

4.1 *Influence of Loose Layer Position on the Monopile H–y Response*

Figure 5 illustrates the H–y/D response curves for ten monopile models embedded in a flat seabed, each characterized by varying positions and thicknesses of the loose sand layer. The initial stiffness was quantified at a displacement of 0.001D, whereas the ultimate capacity was defined at a displacement of 0.1D. The pivot depth (z/L) indicates the depth of the pile's rotation point.

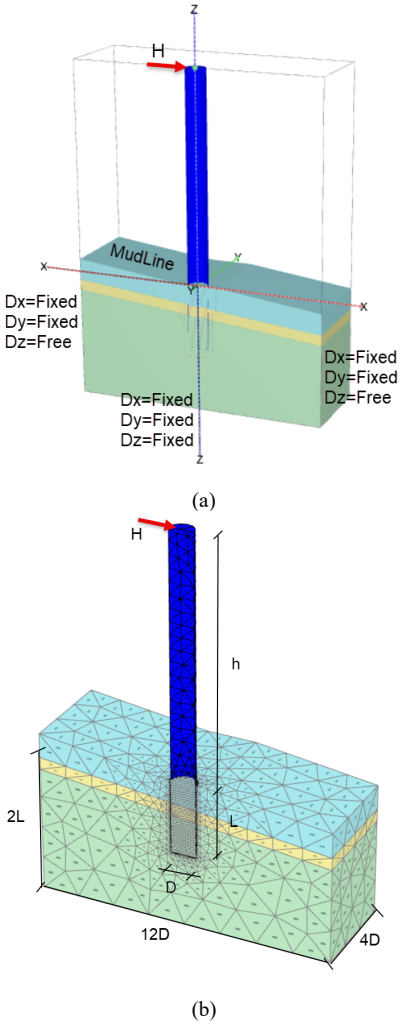

Figure 3. (a) 3D numerical model, and (b) Mesh configuration created for the 3D FE modeling.

For the reference model (F1_Hom), which represents a flat and homogeneous sandy seabed, the initial stiffness is 386.81 MN/m, the ultimate lateral capacity is 44.45 MN, and the pivot depth is located at z/L=0.694 (~0.7).

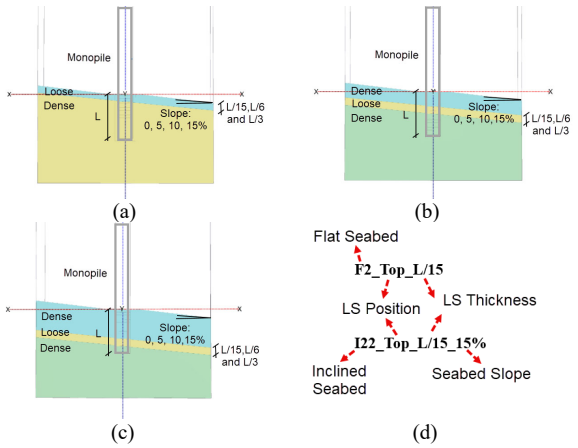

Figure 4. Loose sand position, (a) in the top third layer, (b) in the middle third layer, (c) in the bottom third layer, d) definition of model configurations.

When a loose sand layer is placed at the top (F2–F4), increasing its thickness from L/15 to L/3 (F2_Top_L/15, F3_Top_L/6 and F4_Top_L/3) results in a reduction of stiffness from 369.48 MN/m to 349.91 MN/m and a decrease in ultimate capacity from 42.26 MN to 35.20 MN.

Table 1. The sand and monopile mechanical properties utilized in parametric analyses.

Parameter	Material		
	Loose Sand (LS)	Dense Sand (DS)	Steel pile
Unit Density, γ' [kN/m³]	9.42	11.78	-
Relative Density, Dr [%]	30	70	-
*Small strain Shear Modulus, G_0 [MN/m²]	151	316.2	-
Internal Friction Angle, φ' [°]	33	39	-
Dilation Angle, ψ' [°]	3	9	-
Lateral earth pressure at rest, K_0^{NC} [-]	0.45	0.37	-
Elastic Modulus, E [GN/m²]	-	-	210
Poisson Ratio, μ [-]	-	-	0.3

*At mid-depth of the layer

The pivot level also deepens from z/L=0.698 to 0.715 (Figure 6), indicating weakened surface resistance and an increased depth of rotation. For the mid-layer loose sand configuration (F5–F7), stiffness unexpectedly increases, reaching up to 435.05 MN/m, while ultimate capacity decreases slightly. The pivot level remains relatively stable, ranging between 0.698 and 0.712. This suggests that loosening the mid-layer may mobilize deeper soil, which enhances stiffness but reduces the peak load. In the case of the bottom-layer loose sand (F8–F10), stiffness remains relatively high, approximately 400–429 MN/m, while ultimate capacity varies, with the lowest value observed in F10 (36.52 MN). The pivot level becomes shallower, up to 0.646, indicating that weakening the bottom layer reduces the depth of rotation, possibly due to diminished confinement. These findings emphasize the importance of soil stratification in offshore foundation design, as it directly influences load transfer and pile-soil interaction.

4.2 *Effect of Seabed Inclination on the Monopile H–y Response*

Figure 7 shows a clear trend showing how increasing slope inclination affects the lateral performance of monopiles embedded in homogeneous sand. The sample F1_Hom, composed of homogeneous sand with a flat surface, serves as

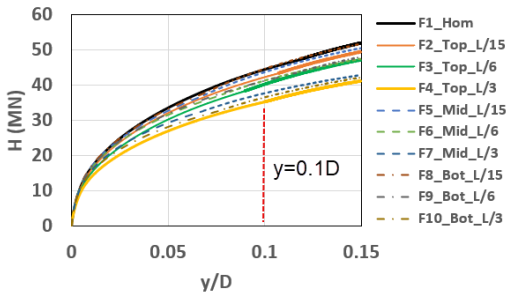

(a)

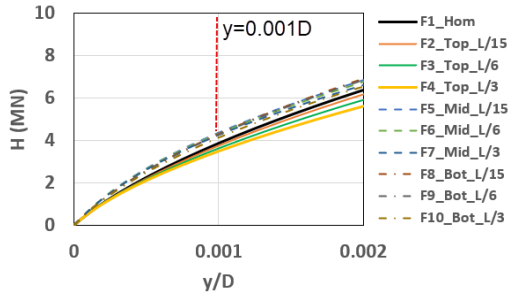

(b)

Figure 5. Comparison of H–y/D curves for monopiles with varying LS layer locations (a) Large displacment, (b) small displacment.

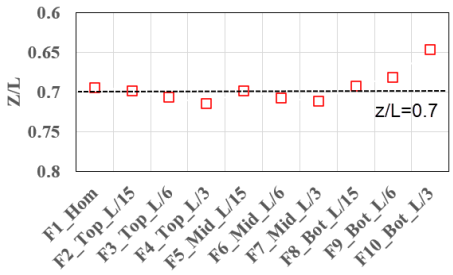

Figure 6. Pivot point depth for varying locations of LS layers.

the reference with the highest initial stiffness (386.81 MN/m) and ultimate capacity (44.45 MN). As the slope increases in samples I1_Hom_5%, I11_Hom_10%, and I21_Hom_15%, both stiffness and capacity show a consistent decline. This reduction correlates with a deeper pivot level, which results in decreased rotation of the monopile at the ground surface for a given head displacemen. Specifically, the pivot level shifts from 0.694 in the flat sample to 0.723 in the 15% inclined sample, while stiffness drops by approximately 7% and capacity by 13%. This indicates that slope inclination reduces lateral resistance and causes the pile to rotate deeper into the soil, likely due to reduced confinement and altered load distribution. These findings highlight the importance of considering seabed geometry in offshore foundation design.

4.3 *Combined Effect of Seabed Inclination and LS Layer Position*

Table 2 presents the initial stiffness, ultimate lateral capacity, and pivot level of monopiles with the LS layer located in the upper third of the embedment depth. The descriptions corresponding to the sample title are presented in Figure 4d. As the seabed slope increases, both the initial stiffness and ultimate capacity decrease, while the pivot level becomes deeper. This effect becomes more pronounced beyond a 5% slope. For the case with a loose layer thickness of L/6, the trend is similar to that observed for L/15, but with slightly lower stiffness and capacity overall due to the thicker loose layer. In the case of L/3, which represents the thickest loose layer in top third length, the reduction in stiffness and capacity is the most significant, and the pivot level reaches its greatest depth, particularly at higher slopes.

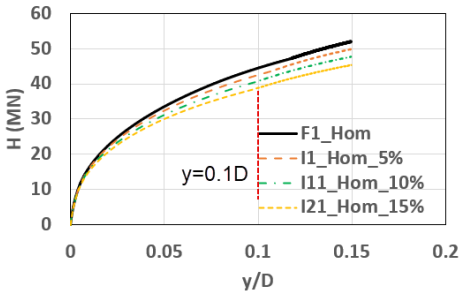

(a)

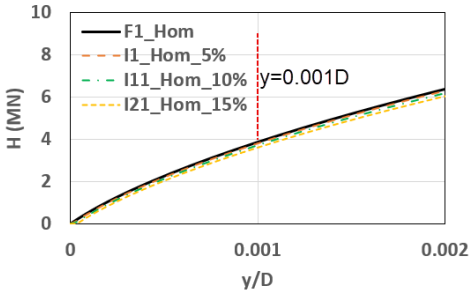

(b)

Figure 7. Comparison of H–y/D curves for monopiles under flat and sloping seabed conditions, (a) Large displacment, (b) small displacment.

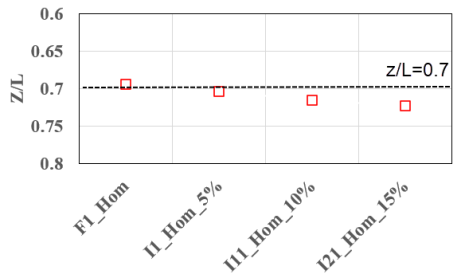

Figure 8. Pivot point depth for varying seabed inclination.

Table 2. Initial stiffness, ultimate lateral capacity and pivot level of monopiles with LS located in the top third of the embedded length.

Sample	Initial Stiffness	Stiffness Ratio	Ultimate Capacity	Capacity ratio	Pivot Level, (z/L)
	(MN/m)	[-]	(MN)	[-]	[-]
F2_Top_L/15	369.48	1.00	42.26	1.00	0.698
I2_Top_L/15_5%	369.20	1.00	42.23	1.00	0.699
I12_Top_L/15_10%	353.40	0.95	38.54	0.91	0.721
I22_Top_L/15_15%	352.90	0.95	36.55	0.86	0.732
F3_Top_L/6	356.79	1.00	40.23	1.00	0.706
I3_Top_L/6_5%	356.91	1.00	38.41	0.95	0.714
I13_Top_L/6_10%	344.35	0.96	36.71	0.91	0.724
I23_Top_L/6_15%	334.03	0.93	34.47	0.85	0.736
F4_Top_L/3	349.91	1.00	35.20	1.00	0.715
I4_Top_L/3_5%	337.74	0.96	34.32	0.97	0.726
I14_Top_L/3_10%	330.32	0.94	32.68	0.92	0.737
I24_Top_L/3_15%	320.07	0.91	30.99	0.88	0.746

Table 3 presents the initial stiffness, ultimate lateral capacity, and pivot level of monopiles with the LS layer located in the middle third of the embedment depth. The findings show that variations in slope inclination and the mid-depth LS layer thickness significantly impact monopile behavior. Unlike top-layer configurations, mid-layer loose sand maintains relatively high initial stiffness, even as slope increases. For example, the reference model F5_Mid_L/15 starts at 435.05 MN/m, and even at 15% slope (I25_Mid_L/15), stiffness remains above 420 MN/m. However, ultimate capacity consistently declines with slope, and the pivot level deepens, indicating decreased pile rotation. Thicker mid-layers (L/3) show slightly lower stiffness and capacity overall, with the deepest pivot levels reaching 0.737. These results suggest that while mid-layer loosening allows deeper soil mobilization (enhancing stiffness), slope inclination still reduces lateral resistance and increases rotation depth. This highlights the complex interaction between soil layering and seabed geometry in offshore pile design.

Table 3. Initial stiffness, ultimate lateral capacity, and pivot level of monopiles with LS located in the middle third of the embedded length.

Sample	Initial Stiffness	Stiffness Ratio	Ultimate Capacity	Capacity ratio	Pivot Level, (z/L)
	(MN/m)	[-]	(MN)	[-]	[-]
F5_Mid_L/15	435.05	1.00	43.71	1.00	0.698
I5_Mid_L/15_5%	432.25	0.99	42.34	0.96	0.708
I15_Mid_L/15_10%	427.41	0.98	40.23	0.92	0.716
I25_Mid_L/15_15%	420.19	0.96	38.14	0.87	0.727
F6_Mid_L/6	432.28	1.00	41.31	1.00	0.706
I6_Mid_L/6_5%	430.05	0.99	39.99	0.96	0.714
I16_Mid_L/6_10%	426.15	0.98	38.08	0.92	0.722
I26_Mid_L/6_15%	418.92	0.96	36.57	0.88	0.734
F7_Mid_L/3	425.21	1.00	37.72	1.00	0.712
I7_Mid_L/3_5%	423.05	0.99	36.22	0.96	0.722
I17_Mid_L/3_10%	419.86	0.98	34.72	0.92	0.729
I27_Mid_L/3_15%	413.16	0.97	33.39	0.88	0.736

Table 4 reports the initial stiffness, ultimate lateral capacity, and pivot level of monopiles with the LS layer located in the bottom third of monopile. The data shows that bottom-layer loose sand configurations maintain relatively high initial stiffness and ultimate capacity, especially in the thinner layers (L/15 and L/6). The reference model F8_Bot_L/15 starts with 429.33 MN/m stiffness and 44.65 MN capacity, with a pivot level at 0.692. As slope increases, both stiffness and capacity gradually decline, and the pivot level deepens, though less dramatically than in top or mid-layer configurations. The thickest bottom layer (L/3) shows the most significant reduction in performance, with stiffness dropping to ~364 MN/m and capacity to ~32 MN at 15% slope. Interestingly, in models containing bottom loose layers, the pivot level tends to occur at shallower depths compared with the top- or mid-loose-layer configurations. This suggests that reduced stiffness at the base diminishes confinement and shifts the rotation point closer to the surface. These results highlight that bottom-layer positioning can preserve stiffness better than other configurations, but slope still plays a critical role in reducing lateral resistance.

The data across all three tables clearly demonstrate that both slope inclination and loose sand layer thickness significantly impact monopile performance. For each thickness level (L/15, L/6, L/3), increasing slope leads to a consistent reduction in initial stiffness and ultimate capacity, while the pivot level becomes deeper.

Table 4. Initial stiffness, ultimate lateral capacity, and pivot level of monopiles with LS located in the bottom third of the embedded length.

Sample	Initial Stiffness	Stiffness Ratio	Ultimate Capacity	Capacity ratio	Pivot Level, (z/L)
	(MN/m)	[-]	(MN)	[-]	[-]
F8_Bot_L/15	429.33	1.00	44.65	1.00	0.692
I8_Bot_L/15_5%	416.43	0.96	42.59	0.95	0.701
I18_Bot_L/15_10%	408.77	0.95	40.23	0.90	0.712
I28_Bot_L/15_15%	404.99	0.94	38.47	0.86	0.722
F9_Bot_L/6	424.86	1.00	41.27	1.00	0.681
I9_Bot_L/6_5%	411.83	0.96	40.90	0.99	0.690
I19_Bot_L/6_10%	410.72	0.96	38.73	0.93	0.702
I29_Bot_L/6_15%	400.08	0.95	37.22	0.90	0.711
F10_Bot_L/3	400.00	1.00	36.52	1.00	0.646
I10_Bot_L/3_5%	408.33	1.02	35.64	0.97	0.654
I20_Bot_L/3_10%	400.34	1.00	33.97	0.93	0.666
I30_Bot_L/3_15%	382.36	0.95	32.44	0.88	0.676

The effect is more pronounced with thicker loose layers, indicating that surface instability and reduced confinement near the pile head contribute to decreased rotation and reduced lateral resistance. These findings emphasize the need to carefully evaluate seabed geometry and soil layering in offshore foundation design, especially in sloped terrains with weak surface layers.

4.4 *Influence of LS Layers and Seabed Inclination on Soil Reaction*

Figure 9a shows the ultimate soil reaction (pu) profiles along the monopile in homogeneous sand for varying seabed slopes. To enable comparison, the API profile is also included in this figure. The API (2014) guideline provides a conservative baseline, with soil reactions generally lower than those obtained from the numerical simulations. The F1_Hom case, representing a flat mudline with homogeneous sand, exhibits the highest soil reaction values, particularly near the upper portion of the monopile, indicating strong lateral resistance. As the seabed slope increases, the cases I1_Hom_5%, I11_Hom_10%, and I21_Hom_15% demonstrate progressively lower soil reactions. The corresponding curves shift leftward, reflecting reduced resistance at each depth up to z/L=0.4. Additionally, the depth of maximum reaction moves slightly downward, suggesting deeper mobilization of soil under inclined seabed conditions.

Figure 9b compares the ultimate soil reaction (pu) profiles along the monopile in homogeneous (F1_Hom) sand and in samples with the loose sand layer at varying positions with maximum thickness (L/3). The F1_Hom case demonstrates the highest pu values, particularly near the surface, indicating strong lateral resistance. When a loose sand layer is introduced at the top (F4_Top_L/3), the pu response near the upper portion of the pile decreases significantly, confirming surface weakening. For the mid-depth loose layer configuration (F7_Mid_L/3), the pu values remain higher than those in F4 but still lower than F1, with a more evenly distributed reaction profile. Finally, in the bottom loose layer case (F10_Bot_L/3), the pu values near the surface are comparable to F1, but they decrease at greater depths, indicating that bottom-layer weakening primarily affects deeper soil mobilization.

This graph illustrates the influence of loose sand layer position on the soil's lateral resistance. Compared to the reference case (F1_Hom), all heterogeneous configurations exhibit deviations. Weakening the top layer results in the largest reduction of pu near the surface.

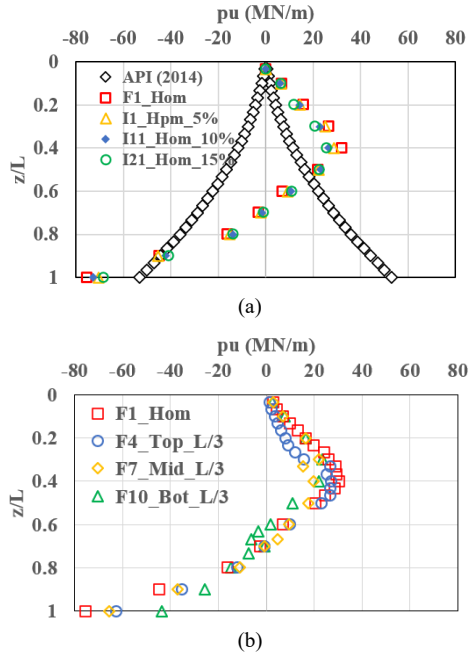

Figure 9. Distribution of pu along the monopile: (a) homogeneous sand under varying seabed slopes, and (b) flat seabed with a LS layer of thickness L/3 positioned at different depths.

Mid-layer configurations provide a more uniform distribution of lateral resistance, whereas bottom-layer configurations maintain surface resistance but limit deeper mobilization. The findings reinforce the need to consider soil stratification and depth-dependent behavior in offshore geotechnical engineering.

5 CONCLUSIONS

The compiled data from forty FE simulations of monopile systems in PLAXIS reveals a consistent and quantifiable relationship between seabed slope, loose sand layer configuration, and lateral pile performance. Across all configurations, including flat and inclined seabed as well as layered sand, the initial stiffness, ultimate lateral capacity, and pivot depth are sensitive to both the position and thickness of the loose sand layer. Flat seabed conditions with homogeneous sand exhibit the highest performance, while increasing slope and loose layer thickness lead to reduced stiffness and capacity, and deeper pivot levels. Notably, top-layer weakening causes the most significant degradation in performance, while mid-depth loose layer configurations maintain higher stiffness but still suffer capacity loss. The models with loose sand at the bottom exhibit better stiffness preservation and display shallower pivot depths, indicating reduced rotational demand; however, they still experience a decrease in lateral capacity under sloping conditions. These trends highlight the importance of soil stratification and seabed geometry in offshore monopile design, where slope-induced instability and weak zones can critically affect load transfer and rotational behavior.

6 REFERENCES

American Petroleum Institute (API), 2014. Petroleum and natural gas industries-specific requirements for offshore structures. Part 4 – Geotechnical and foundation design considerations ISO 19901-4:2003 (Modified).

Bentley Systems, 2024. PLAXIS 3D [Computer software]. Bentley Systems Incorporated. https://www.bentley.com

Benz, T., 2007. Small-Strain Stiffness of Soils and its Numerical Consequences. Dissertation, Universität Stuttgart.

Byrne, B.W., Houlsby, G.T., Burd, H.J., Gavin, K.G., Igoe, D.J., Jardine, R.J., Martin, C.M., McAdam, R.A., Potts, D.M., Taborda, D.M., Zdravković, L., 2020. PISA design model for monopiles for offshore wind turbines: application to a stiff glacial clay till. *Géotechnique* 70(11), 1030–1047.

Chae, K., Ugai, K., Wakai, A., 2004. Lateral resistance of short single piles and pile groups located near slopes. *Int. J. Geomech*. 4(2), 93–103.

Chandaluri, V.K., Sawant, V.A., 2020. Influence of sloping ground on lateral load capacity of single piles in clayey soil. *Int. J. Geotech. Eng*. 14(4), 353–360.

Gabr, M.A., Borden, R.H., 1990. Lateral analysis of piers constructed on slopes. *J. Geotech. Eng*. 116(12), 1831–1850.

Georgiadis, K., Georgiadis, M., 2010. Undrained lateral pile response in sloping ground. *J. Geotech. Geoenviron. Eng*. 136(11), 1489–1500.

Georgiadis, K., Georgiadis, M., 2012. Development of p–y curves for undrained response of piles near slopes. *Comput. Geotech*. 40, 53–61.

Georgiadis, M., Anagnostopoulos, C., Saflekou, S., 1992. Centrifugal testing of laterally loaded piles in sand. *Can. Geotech. J*. 29(2), 208–216.

Haiderali, A.E., Madabhushi, G.S., 2025. Effect of loose sand layers within dense sand on the lateral capacity of extra-extra-large monopiles. Mar. *Georesources Geotechnol*. 43(7), 1324–1338.

Hu, Q., Han, F., Prezzi, M., Salgado, R., Zhao, M., 2022. Finite-element analysis of the lateral load response of monopiles in layered sand. *J. Geotech. Geoenviron. Eng*. 148(4), 04022001.

Lin, M., Jiang, C., Liu, P., Pang, L., 2022. Analysis of laterally loaded offshore pile near slope in sand considering slope height. *Ocean Eng*. 263, 112436.

Meyerhof, G.G., 1959. Compaction of sands and bearing capacity of piles. *J. Soil Mech. Found. Div*. 85(6), 1–29.

Mezazigh, S., Levacher, D., 1998. Laterally loaded piles in sand: slope effect on p–y reaction curves. *Can. Geotech. J*. 35(3), 433–441.

Mirzoyan, 2007. Lateral resistance of piles at the crest of slopes in sand. Brigham Young University.

Muthukkumaran, K., 2014. Effect of slope and loading direction on laterally loaded piles in cohesionless soil. *Int. J. Geomech*. 14(1), 1–7.

Muthukkumaran, K., Sundaravadivelu, R., Gandhi, S.R., 2008. Effect of slope on p–y curves due to surcharge load. *Soils Found*. 48(3), 353–361.

Nimityongskul, N., Kawamata, Y., Rayamajhi, D., et al., 2017. Full-scale tests on effects of slope on lateral capacity of piles installed in cohesive soils. J. *Geotech. Geoenviron. Eng*. 144(1), 04017103.

Peng, W., Zhao, M., Xiao, Y., Yang, C., Zhao, H., 2019. Analysis of laterally loaded piles in sloping ground using a modified strain wedge model. *Comput. Geotech*. 107, 163–175.

Poulos, H.G., Hull, T.S., 1989. The role of analytical geomechanics in foundation engineering. In: Foundation Engineering @Current Principles and Practices. ASCE, pp. 1578–1606.

Reese, L.C., Cox, W.R., Koop, F.D., 1974. Analysis of laterally loaded piles in sand. In: Offshore Technology Conference, OTC-2080.

Sánchez, S., López-Gutiérrez, J.S., Negro, V., Esteban, M.D., 2019. Foundations in offshore wind farms: evolution, characteristics and range of use. Analysis of main dimensional parameters in monopile foundations. *J. Mar. Sci. Eng*. 7(12), 441.

Sivapriya, S., Gandhi, S., 2011. Behaviour of single pile in sloping ground under static lateral load. In: *Proceedings of Indian Geotechnical Conference*, pp. 199–202.

Yue, S., Zhang, L., Zhou, S., Peng, W., Wu, G., Zhao, M., 2024. Experimental investigation into effects of slope and loading characteristics on cyclic laterally loaded monopile in sand. *Ocean Eng*. 294, 116784.